

On the Cepheid variables of nearby galaxies III. NGC 3109

Ilaria Musella

Osservatorio Astronomico di Capodimonte, via Moiariello 16,
I-80131 Napoli, Italy

Giampaolo Piotto

Dipartimento di Astronomia, Università di Padova, I-35122 Padova, Italy

Massimo Capaccioli

Osservatorio Astronomico di Capodimonte, salita Moiariello 16,
I-80131 Napoli, Italy

and

Dipartimento di Scienze Fisiche, Università di Napoli
Mostra d'Oltremare, Padiglione 19, I-80125–Italy

ABSTRACT

We extended to the R and I bands the light curve coverage for 8 Cepheids already studied in B and V by Capaccioli *et al.* [AJ, 103, 1151 (1992)]. Sixteen additional Cepheid candidates have been identified and preliminary periods are proposed. The new Cepheids allow the period-luminosity relation to be extended one magnitude fainter. Apparent B, V, R, and I distance moduli have been calculated. Combining the data at different wavelengths, and assuming a true distance modulus of 18.50 mag for the LMC, we obtain for NGC 3109 a true distance modulus $(m - M)_0 = 25.67 \pm 0.16$, corresponding to 1.36 ± 0.10 Mpc. Adopting $E(B - V) = 0.08$ for the LMC, the interstellar reddening for the Cepheids in NGC 3109 is consistent with 0. A discussion on the possible implications of this result is presented. A comparison of the period-color, period-amplitude, and period-luminosity relations suggests similar properties for the Cepheids in the LMC, NGC 3109, Sextans A, Sextans B, and IC 1613, though the uncertainties in the main parameter determination are still unsatisfactorily high for a firm conclusion on the universality of the period-luminosity relation.

Subject headings: Cepheids — galaxies: distances and redshifts — galaxies: individual (NGC 3109)

1. Introduction

This paper is part of a program aimed at increasing the number of galaxies with accurate distance determinations via ground-based multicolor CCD photometry of Cepheid variables.

In the first paper of the series, Capaccioli, Piotto and Bresolin (1991, CPB) presented new BV photometry of the Cepheids belonging to the sample of variables already identified by Sandage and Carlson (1988, SC) in NGC 3109. In that work, CPB derived a new zero point for the photometric scale. The new data gave a distance modulus $\mu_0 = 25.5$ mag, $\sim 25\%$ shorter than previously measured by SC. The availability of only two photometric bands (B and V) did not allow CPB to apply the multicolor method discussed by Freedman (1985, F85) to directly estimate the internal absorption of the Cepheids in NGC 3109. Actually, Bresolin, Capaccioli, and Piotto (1993, BCP) pointed out that the internal absorption in some of the fields studied by CPB could be greater than the adopted average value $E(B-V)=0.04$. Besides improving the photometry of the Cepheids previously discovered on photographic plates, CCD data allow us also to obtain more accurate and deeper photometry in crowded fields, enabling the discovery of new fainter Cepheids. The consequent extension of the period–luminosity relation (PL) to shorter periods permits a more accurate determination of its zero point. For instance, in the second paper of this series, Piotto, Capaccioli and Pellegrini (1994, PCP) found five new Cepheids in Sextans A and four in Sextans B, in addition to the five variables in Sextans A and the three in Sextans B already discovered by Sandage and Carlson (1982, 1985). The new variables extended the faint end of the PL relation of these two galaxies by one magnitude. PCP observed these two galaxies in three passbands: B , V and I , again obtaining a new zero point for the photometric calibration. Using the multiwavelength photometry method (F85) they derived a true distance modulus, corrected for interstellar extinction, of $\mu_0 = 25.71$ for Sextans A and of $\mu_0 = 25.63$ for Sextans B, assuming a distance modulus $\mu_0 = 18.50$ for the Large Magellanic Cloud (LMC).

In the framework of this program, here we present a new determination of the distance to the galaxy NGC 3109 based on a new $BVRI$ photometry of the Cepheids located in the field F1 of BCP. The data set and the reduction procedures are illustrated in the Section 2. In Section 3 we present the already known variables and our 16 new Cepheid candidates on which the present distance determination of NGC 3109 is based. The determination of the Cepheid parameters is discussed in Section 4, while Section 5 is devoted to the determination of the distance to NGC 3109. A comparison of the PL and period-color relations for the Cepheids in a few nearby galaxies is presented in Section 6. A brief discussion and a comparison with the previous determinations of the distance to NGC 3109 is in Section 7.

2. Observations and Reductions

This study is a follow up of the work by CPB. In that paper it was impossible to identify new Cepheids due to the limited time coverage and small number of data points (six at most). We then collected, in December 1991, March 1992 and February 1993, a series of B , V , R , and I -band images of a $1'.9 \times 3'.0$ field (Fig. 1) of NGC 3109 coded as F1 (*cf.* Table 1 for the log of the observations).

The I and R band images of December 1991 were taken with EFOSC2 + CCD #17 at the ESO/MPI 2.2m telescope at La Silla in Chile. The CCD format is 1024×1024 pixels of $0''.332$. The set of the B , V , and R band images of March 1992 was obtained with the RCA #8 CCD camera at the Cassegrain focus of the ESO/MPI 2.2m telescope with a CCD format of 640×1024 pixels and a pixel size of $0''.175$. Furthermore, three B -band frames at the blue arm of EMMI equipped with the Tektronix #31 CCD and one in the I -band at the red arm of EMMI with the Tektronix #18 CCD have been collected at the ESO-NTT telescope on February, 1993. CCD dimensions is 1024×1024 pixels and the pixel sizes in blue and red are $0''.370$ and $0''.290$ respectively.

During these observing runs, at least thirteen Landolt's (1983a,b) standard stars were observed in each color in order to transform the instrumental photometry into the Landolt standard system.

A large set of bias, dark, and flat field frames have been collected, particularly during the observing runs at the 2.2m telescope. Indeed, the columns of the high resolution ESO-RCA chip #8 have not a constant bias as it depends on the total intensity of the light which falls over the column. The procedure used for the image cleaning and calibration is as in PCP and Pellegrini (1993).

The CCD data have been reduced with DAOPHOT and ALLSTAR. Particular attention has been devoted in tying the stellar photometry to Landolt's (1983a,b) standard system. For the calibration of the B and V colors we used the previous CPB calibration, while for the calibration of the R -band and I -band we observed 16 Landolt (1983a,b) standard stars in each color in December of 1991 and 13 Landolt standard stars for the I band in February of 1993. As in Piotto et al. (1990), in order to obtain the R_{1991} , I_{1991} and I_{1993} calibrated magnitudes we adopted linear color terms. For the calibration of the R_{1992} magnitudes we applied the same calibration parameters of R_{1991} , after having obtained the linear relation between R_{1991} and R_{1992} . The uncertainty on the calibration of the B and V photometry is 0.03 mag. This value represents the combination of the error in the CPB calibration and of the error on the zero point difference between our photometry and that of CPB. For the R and I bands we obtained a zero point error in the calibration equation of 0.01 mag. However, the largest error source in the calibration procedure comes from the transformation of the zero point of the point-spread-function (PSF) fitting photometry of NGC 3109 stars into the standard star aperture photometry zero point (CPB). In our

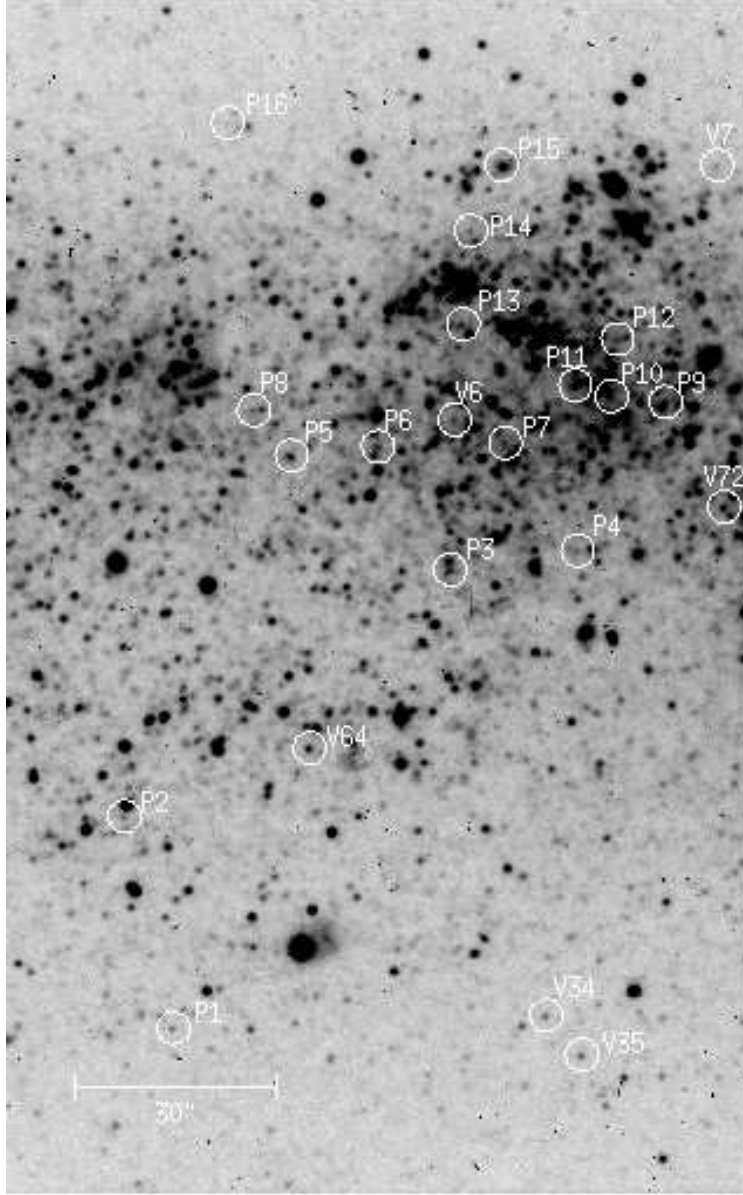


Fig. 1.— *B*-band CCD image (2.2m telescope, 40 min exposure) of the field F1 in NGC 3109. North is up, East to the right. The Cepheids are marked by a circle. The stars coded as V belong to the original SC sample, while P refers to the new candidate Cepheids.

frames all of the stars are distributed over a very inhomogeneous background, making the aperture photometry quite uncertain. For the I band we have two independent calibrations (one from the 2.2m telescope and one from the NTT telescope). The average zero point differences from night to night were of 0.05 mag. The same (average) zero point calibration has been adopted for the two I frames. In R we could not use the same method, since the calibration equation was available for one night only. For R_{1991} we obtained an error of 0.05 mag on the difference between the aperture photometry and the PSF fitting photometry. Finally, we obtained an uncertainty of 0.07 mag on the calibration of the R_{1992} magnitude determinations summing the error on the linear relation between R_{1991} and R_{1992} magnitudes to the calibration error of the R_{1991} calibration. Throughout the paper, whenever needed, we took into proper account the fact that the zero point calibration of R_{1991} is more accurate than the R_{1992} one. The calibration zero point errors for each image are reported in Table 1, Col. 5.

The internal error on the photometry can be easily evaluated by comparing the independent magnitude determinations of the not variable stars in each color. For each color, Table 2, gives the mean internal errors (identified with *error*, Cols. 2, 4, 6 and 8) and the number of stars (identified with *stars*, Cols. 3, 5, 7 and 9) at different magnitude intervals (Col. 1) in the four photometric bands. The accuracy of the CCD light curves of the Cepheids can be obtained from the uncertainties quoted in this Table.

3. Cepheids in NGC 3109

3.1. Cepheids in common with previous studies

SC have identified 29 Cepheids in NGC 3109. CPB selected only 21 of them, excluding candidate Cepheids with high photometric uncertainties or those that did not show significant light variations during the period covered by their observations (*cf.* CPB for more details). This work is based on the same selection of 21 Cepheids. Six of them (marked as V in Fig. 1) fall in field F1 monitored in the present study. As in CPB, we applied a zero point shift of -0.29 mag to the SC data (SC data are fainter). The new CCD data in the B -band for the six Cepheids located in the field F1 were plotted together with CPB and SC photometry, and the periods were interactively adjusted in order to obtain the best phase match among these three data sets. The new, complete light curves of these six Cepheids are reproduced in Fig. 2. Differences between our and CPB periods are very small, $\sim 10^{-2}$ days for V72 and $\sim 10^{-4}$ days for the other variables (*cf.* Table 5).

For each of these variables, we could also add another point in the V -band light curve, and one or two magnitude determinations in the I and R bands. In addition, also SC V36 and V45 variables fall within our larger R and I frames, allowing us to measure their R and I magnitudes. The new magnitude determinations for the SC Cepheids are reported in the

Table 1. Log book of the observations.

Date	Band	Exp. time [min]	Seeing FWHM	calib. err. ^A
1-12-1991	I ^B	24	1'.14	0.05
1-12-1991	R	12	1'.02	0.05
1-03-1992	B	40	1'.17	0.03
1-03-1992	V	20	1'.16	0.03
2-03-1992	B	40	1'.32	0.03
3-03-1992	B	40	1'.12	0.03
7-03-1992	B	40	0'.87	0.03
8-03-1992	B	40	1'.30	0.03
9-03-1992	B	40	0'.80	0.03
9-03-1992	R	18	0'.94	0.07
17-02-1993	B	30	1'.30	0.03
18-02-1993	B	30	1'.00	0.03
20-02-1993	B	25	1'.60	0.03
20-02-1993	I	13	1'.20	0.05

^AThis is the total error on the calibration (see text for details)

^BThis image is a sum of two images each one with an exposition time of 12 min.

Table 2. Photometric internal errors in the B, V, R and I bands.

Mag	B		V		R		I	
	Error	Stars	Error	Stars	Error	Stars	Error	Stars
19.75	0.04	12	0.02	23	0.02	42	0.02	55
20.25	0.04	28	0.04	38	0.03	66	0.03	84
20.75	0.04	83	0.04	108	0.04	140	0.04	121
21.25	0.04	118	0.05	172	0.05	150	0.06	121
21.75	0.05	157	0.06	208	0.06	163	0.08	95
22.25	0.06	189	0.07	227	0.10	76	0.12	17
22.75	0.07	192	0.09	136	0.20	18	0.29	8
23.25	0.08	134	0.14	50	–	–	–	–
23.75	0.13	33	0.30	6	–	–	–	–
24.25	0.17	8	0.32	1	–	–	–	–

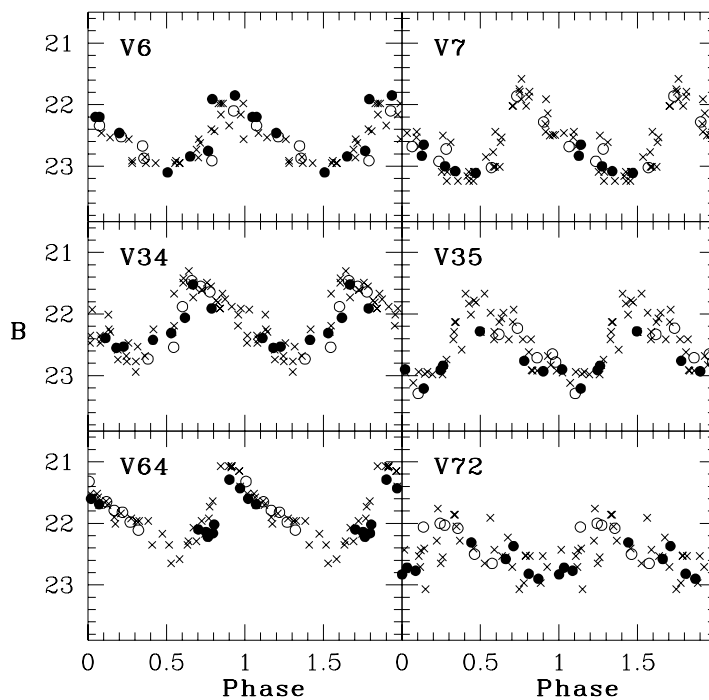


Fig. 2.— Light curves for the six Cepheid variables identified by SC in field F1. *Crosses* represent the original SC photometry, shifted by $\Delta B = 0.29$ mag (CPB). The *Open circles* represent the CPB data and the *filled circles* the new data presented in this paper.

Table 3.

3.2. New candidate Cepheids

In order to search for new candidate Cepheid variables, we used both CPB raw data and the photometry presented in this paper. We computed for each star, for both the B and V magnitude determinations, the *normalized* standard deviation (σ_N), i.e. the standard deviation divided by the mean photometric internal error in each magnitude intervals of 0.5 mag. We considered as possible variables only those stars satisfying the relation:

$$\sqrt{\sigma_N^2(B) + \sigma_N^2(V)} \geq 2$$

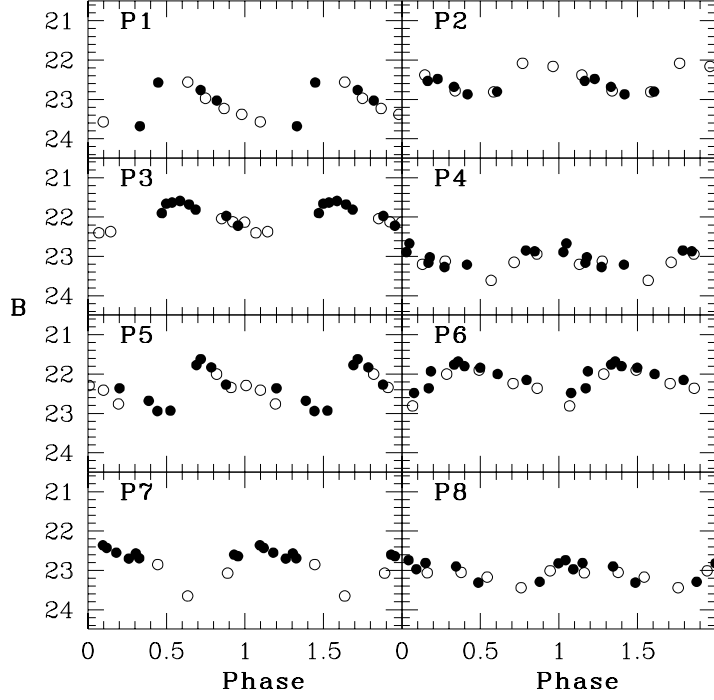
By this procedure, we isolated 129 stars. The possible Cepheids were selected from these candidates on the basis of their light curve, excluding spurious objects in which only one or two points contributed to the large deviation. We ended with a list of 29 stars. Among these there were all the Cepheids previously discovered by SC. Of the remaining variable candidates, only 16 had colors and light curves (after rephasing) typical of a Cepheid¹. The 16 new Cepheid candidates located in field F1 are marked with a circle and coded as P in Fig. 1; their photometry is reported in Table 4. The most probable periods of the new Cepheids have been determined by the usual Fourier analysis. More data are needed to confirm the periods, though the light curves seem well enough covered to allow a fair determination of the parameters of the PL relation. The light curves of these new candidates are plotted with their tentative periods in Fig. 3.

¹($B - V$) colors have proven to be a valuable aid in discriminating Cepheids from other variables, allowing the rejection of many objects with colors differing significantly from those typical of Cepheids (*cf.* also Fig. 11).

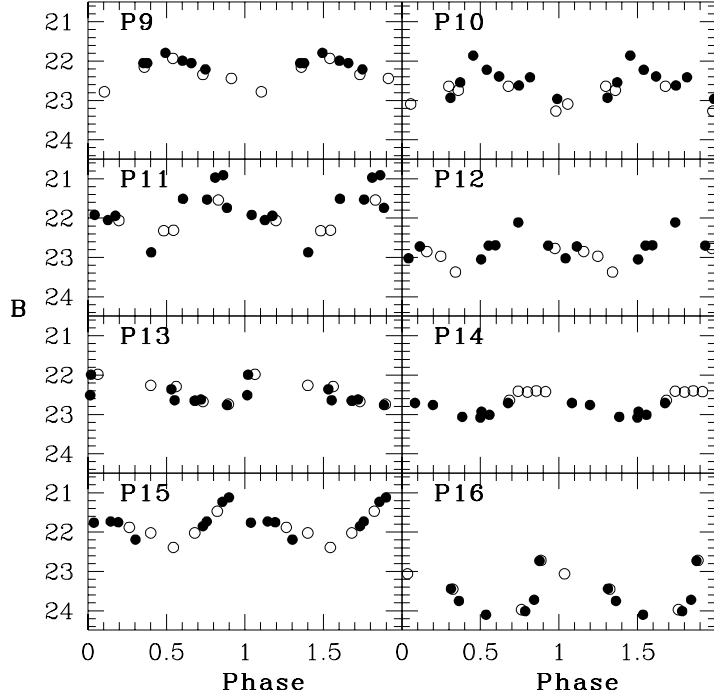
Table 3. SC Cepheids in NGC 3109^A

Julian Date	B	V	R	I	B	V	R	I
V6				V7				
2448591.825	–	–	–	–	–	–	21.13	20.94
8683.579	–	22.37	–	–	22.65	21.92	–	–
8684.779	21.85	–	–	–	23.08	–	–	–
8685.561	22.20	–	–	–	23.11	–	–	–
8688.789	23.10	–	–	–	–	–	–	–
8689.794	22.84	–	–	–	–	–	–	–
8690.786	21.91	–	21.11	–	–	–	21.72	–
9036.804	22.20	–	–	–	22.83	–	–	–
9037.688	22.46	–	–	–	23.00	–	–	–
9039.734	–	–	–	20.90	–	–	–	–
V34				V35				
2448591.825	–	–	20.54	20.27	–	–	21.40	21.20
8683.579	22.39	–	–	–	22.90	22.07	–	–
8684.779	22.55	–	–	–	–	–	–	–
8685.561	22.53	–	–	–	22.84	–	–	–
8688.789	22.42	–	–	–	–	–	–	–
8689.794	–	–	–	–	22.76	–	–	–
8690.786	22.31	–	20.42	–	22.93	–	22.66	–
9036.804	22.06	–	–	–	23.21	–	–	–
9037.688	21.52	–	–	–	22.91	–	–	–
9039.734	21.91	–	–	20.00	22.28	–	–	21.08
V64				V72				
2448591.825	–	–	20.22	19.90	–	–	22.41	21.54
8683.579	22.10	21.18	–	–	22.90	–	–	–
8684.779	22.22	–	–	–	22.83	–	–	–
8685.561	22.02	–	–	–	22.77	–	–	–
8688.789	21.43	–	–	–	22.31	–	–	–
8689.794	21.60	–	–	–	–	–	–	–
8690.786	21.69	–	20.23	–	22.58	–	–	–
9036.804	22.14	–	–	–	22.37	–	–	–
9037.688	22.16	–	–	–	22.82	–	–	–
9039.734	21.29	–	–	19.96	22.72	–	–	–
V36				V45				
2448591.825	–	–	22.41	21.54	–	–	22.50	–
8683.579	–	–	–	–	–	–	–	–
8684.779	–	–	–	–	–	–	–	–
8685.561	–	–	–	–	–	–	–	–
8688.789	–	–	–	–	–	–	–	–
8689.794	–	–	–	–	–	–	–	–
8690.786	–	–	–	–	–	–	–	–
9036.804	–	–	–	–	–	–	–	–
9037.688	–	–	–	–	–	–	–	–
9039.734	–	–	–	–	–	–	–	–

^AFor CPB data see their Table 3(a).



a)



b)

Fig. 3.— a), b): The Light curves for the 16 new candidate Cepheid variables with a tentative period identification (*cf.* Table 5). The *open circles* represent the CPB's data, while the

Table 4. New candidate Cepheids in NGC 3109: CPB and our data.

Julian Date	B	V	R	I	B	V	R	I
P1				P2				
2447967.588	22.56	22.02	–	–	22.81	22.40	–	–
7968.559	22.97	22.14	–	–	22.08	21.88	–	–
7969.581	23.23	22.44	–	–	22.16	21.98	–	–
7970.551	23.38	22.49	–	–	22.38	22.02	–	–
7971.570	23.57	22.63	–	–	22.78	22.36	–	–
8591.825	–	–	22.30	22.07	–	–	22.01	–
8683.579	–	–	–	–	–	–	–	–
8684.779	–	–	–	–	–	–	–	–
8685.561	–	–	–	–	–	–	–	–
8688.789	23.68	–	–	–	22.48	–	–	–
8689.794	22.57	–	–	–	22.87	–	–	–
8690.786	–	–	–	–	22.80	–	–	–
9036.804	22.76	–	–	–	22.53	–	–	–
9037.688	23.03	–	–	–	22.68	–	–	–
9039.734	–	–	–	21.90	–	–	–	21.83
P3				P4				
2447967.588	22.04	21.27	–	–	22.94	23.16	–	–
7968.559	22.12	21.28	–	–	23.12	–	–	–
7969.581	22.13	–	–	–	23.15	–	–	–
7970.551	22.40	21.40	–	–	23.20	22.83	–	–
7971.570	22.37	21.55	–	–	23.61	23.03	–	–
8591.825	–	–	20.65	20.42	–	–	–	–
8683.579	21.66	20.97	–	–	23.02	–	–	–
8684.779	21.59	–	–	–	–	–	–	–
8685.561	21.68	–	–	–	22.89	–	–	–
8688.789	21.97	–	–	–	23.21	–	–	–
8689.794	22.22	–	–	–	22.87	–	–	–
8690.786	–	–	20.94	–	23.27	–	–	–
9036.804	21.90	–	–	–	22.85	–	–	–
9037.688	21.63	–	–	–	23.16	–	–	–
9039.734	21.81	–	–	20.36	22.67	–	–	–
P5				P6				
2447967.588	22.00	21.29	–	–	22.36	21.91	–	–
7968.559	22.34	21.53	–	–	22.81	21.95	–	–
7969.581	22.29	21.51	–	–	22.00	21.51	–	–
7970.551	22.41	–	–	–	21.90	21.70	–	–
7971.570	22.76	21.96	–	–	22.24	21.69	–	–
8591.825	–	–	–	20.74	–	–	21.36	21.00
8683.579	22.36	21.55	–	–	22.48	–	–	–
8684.779	–	–	–	–	21.76	–	–	–
8685.561	22.68	–	–	–	21.84	–	–	–
8688.789	21.77	–	–	–	21.93	–	–	–
8689.794	21.83	–	–	–	21.80	–	–	–
8690.786	22.27	–	21.07	–	22.00	–	21.37	–
9036.804	22.94	–	–	–	22.36	–	–	–
9037.688	22.93	–	–	–	21.68	–	–	–
9039.734	21.62	–	–	20.64	22.15	–	–	21.04

Table 4—Continued

Julian Date	B	V	R	I	B	V	R	I
P7					P8			
2447967.588	23.07	21.71	—	—	23.05	22.64	—	—
7968.559	—	—	—	—	23.44	—	—	—
7969.581	—	21.62	—	—	23.06	22.84	—	—
7970.551	22.85	21.64	—	—	23.17	—	—	—
7971.570	23.65	21.59	—	—	23.01	23.02	—	—
8683.579	22.64	21.48	—	—	22.74	—	—	—
8684.779	22.55	—	—	—	—	—	—	—
8685.561	22.69	—	—	—	—	—	—	—
8688.789	22.60	—	—	—	22.97	—	—	—
8689.794	22.43	—	—	—	23.31	—	—	—
8690.786	22.57	—	—	—	23.29	—	—	—
9036.804	22.36	—	—	—	22.82	—	—	—
9037.688	22.70	—	—	—	22.90	—	—	—
9039.734	—	—	—	—	22.81	—	—	—
P9					P10			
2447967.588	22.15	21.69	—	—	23.09	—	—	—
7968.559	21.93	—	—	—	22.74	—	—	—
7969.581	22.34	—	—	—	22.64	21.69	—	—
7970.551	22.44	21.76	—	—	23.27	21.91	—	—
7971.570	22.78	21.80	—	—	22.64	21.66	—	—
8591.825	—	—	21.00	—	—	—	—	20.48
8683.579	22.05	21.50	—	—	22.54	21.61	—	—
8684.779	21.99	—	—	—	22.62	—	—	—
8685.561	22.21	—	—	—	22.96	—	—	—
8688.789	22.05	—	—	—	—	—	—	—
8689.794	—	—	—	—	22.93	—	—	—
8690.786	—	—	20.99	—	22.39	—	21.29	—
9036.804	21.79	—	—	—	22.22	—	—	—
9037.688	22.05	—	—	—	22.41	—	—	—
9039.734	—	—	—	20.77	21.86	—	—	20.35
P11					P12			
2447967.588	22.32	21.59	—	—	22.77	—	—	—
7968.559	21.54	21.01	—	—	—	—	—	—
7969.581	22.06	22.12	—	—	22.85	22.74	—	—
7970.551	22.31	21.78	—	—	22.97	22.98	—	—
7971.570	—	21.59	—	—	23.37	22.92	—	—
8591.825	—	—	—	—	—	—	22.49	—
8683.579	21.94	21.73	—	—	22.70	22.32	—	—
8684.779	21.51	—	—	—	23.02	—	—	—
8685.561	21.74	—	—	—	22.72	—	—	—
8688.789	21.92	—	—	—	—	—	—	—
8689.794	22.87	—	—	—	23.05	—	—	—
8690.786	21.53	—	21.38	—	22.69	—	22.24	—
9036.804	20.97	—	—	—	—	—	—	—
9037.688	22.05	—	—	—	22.70	—	—	—
9039.734	20.91	—	—	—	22.11	—	—	—

4. Cepheid parameters

The old photographic and the new CCD B -band data provide a good coverage of the blue light curves. It is therefore straightforward to derive the magnitudes at maximum (B_{max}) and the mean magnitudes ($\langle B \rangle$) listed in Cols. 4 and 5 of Table 5. The parameters for the SC Cepheids have been estimated giving more weight to the CCD than to the photographic photometry, particularly at the minimum light. We also attempted to obtain the phase weighted mean magnitude using the relation (4) in Saha et al. (1994) after transform the magnitudes into intensities. As discussed by Saha & Hoessel (1990), this method takes care of the bias introduced by the loss of faint measurements. Unfortunately, the phase sampling of the light curves is not sufficiently even; thus, we preferred to compute the mean directly from the light curve drawn by hand through the available points and use the phase weighted mean only for a comparison. In order to obtain the mean V -band magnitude we used the same method as for the B -band. These values are reported in Col. 7 of Table 5.

Finally, even though there are only random phase data available in R and I bands, it is always possible to use the information from the blue light curves to correct these observations to the mean $\langle R \rangle$, $\langle I \rangle$ light (Freedman 1988, F88). The Cepheid light curves in blue differ from those at longer wavelength in two respects: (i) the amplitude decreases with increasing wavelength, and (ii) there is a phase shift moving from the B to the I -band. After transforming the blue photographic light curves into the CCD photometric scale, a correction for both the amplitude scale and the phase shift² was applied as in F88 in order to obtain the mean magnitudes for the R and I data (Cols. 9 and 11 of Table 5). Here, we took into proper account that the R_{1991} magnitude determinations are more accurate than the R_{1992} ones.

In order to estimate the uncertainty associated with the mean magnitudes, we considered all the independent sources of errors acting on this quantity: the amplitude of the light curve that was converted into its equivalent variance (see Freedman et al. 1991, 1992), the internal photometric errors, and the zero-point errors in the calibrated magnitudes (see Table 1 and Table 2). For the bands B and V , the total error was obtained adding in quadrature these errors and dividing by the reduced number of degrees of freedom. For the bands R and I , we have so few points (no more than two) that we consider more reasonable assuming as error on the mean magnitudes the half-amplitude of the light curve, as predicted from the B light curve (F88). Obviously, this uncertainty must be considered as an upper limit of the error to be associated to the mean magnitude. The resulting errors are shown in Table 5 Cols. 6,8,10, and 12.

²We have assumed that the amplitude ratios as a function of the color and the phase shift are the same as in Freedman (1988).

Table 4—Continued

Julian Date	B	V	R	I	B	V	R	I
P13				P14				
2447967.588	22.26	21.80	–	–	22.64	22.37	–	–
7968.559	22.29	21.57	–	–	22.41	22.24	–	–
7969.581	22.67	21.78	–	–	22.43	22.08	–	–
7970.551	22.74	22.22	–	–	22.40	22.04	–	–
7971.570	21.98	21.63	–	–	22.42	21.87	–	–
8591.825	–	–	21.35	21.11	–	–	22.20	–
8683.579	22.65	–	–	–	22.71	–	–	–
8684.779	–	–	–	–	–	–	–	–
8685.561	22.51	–	–	–	22.76	–	–	–
8688.789	22.64	–	–	–	23.06	–	–	–
8689.794	22.62	–	–	–	–	–	–	–
8690.786	22.76	–	21.65	–	23.08	–	22.41	–
9036.804	22.36	–	–	–	22.93	–	–	–
9037.688	22.65	–	–	–	23.01	–	–	–
9039.734	21.99	–	–	–	22.71	–	–	20.55
P15				P16				
2447967.588	21.88	21.15	–	–	23.97	23.28	–	–
7968.559	22.02	21.44	–	–	23.06	22.69	–	–
7969.581	22.39	–	–	–	23.45	22.85	–	–
7970.551	22.02	21.42	–	–	–	23.20	–	–
7971.570	21.47	21.09	–	–	22.72	22.33	–	–
8591.825	–	–	21.16	–	–	–	22.51	–
8683.579	–	–	–	–	23.72	23.36	–	–
8684.779	21.75	–	–	–	–	–	–	–
8685.561	22.19	–	–	–	–	–	–	–
8688.789	21.73	–	–	–	23.44	–	–	–
8689.794	21.12	–	–	–	–	–	–	–
8690.786	21.76	–	–	–	22.73	–	–	–
9036.804	21.85	–	–	–	24.10	–	–	–
9037.688	21.23	–	–	–	24.01	–	–	–
9039.734	21.73	–	–	–	23.75	–	–	22.18

Table 5. NGC 3109 Cepheid parameters.

Cepheid Ident	P_{CPB} [days]	P_{our} [days]	B_{max} [mag]	$\langle B \rangle$ [mag]	$\sigma_{\langle B \rangle}$ [mag]	$\langle V \rangle$ [mag]	$\sigma_{\langle V \rangle}$ [mag]	$\langle R \rangle$ [mag]	$\sigma_{\langle R \rangle}^A$ [mag]	$\langle I \rangle$ [mag]	$\sigma_{\langle I \rangle}^A$ [mag]
V6	7.0223	7.02120	21.78	22.46	0.04	21.80	0.04	20.92	0.29	20.77	0.23
V7	5.9879	5.98810	21.71	22.43	0.05	21.98	0.05	21.22	0.32	20.91	0.24
V8	14.4500	–	20.85	21.45	0.10	–	–	–	–	–	–
V9	7.7670	–	22.10	22.90	0.10	21.90	0.10	–	–	–	–
V11	7.9298	–	21.85	22.40	0.10	–	–	–	–	–	–
V12	8.1183	–	21.70	22.43	0.10	21.86	0.10	–	–	–	–
V18	8.3707	–	21.60	22.38	0.10	21.68	0.10	–	–	–	–
V20	8.2718	–	21.90	22.40	0.10	22.20	0.10	–	–	–	–
V34	17.2320	17.22550	21.43	22.12	0.04	21.28	0.05	20.62	0.30	20.12	0.23
V35	8.1928	8.19190	21.65	22.45	0.05	21.80	0.05	21.53	0.35	21.22	0.27
V36	7.1290	–	21.90	22.25	0.10	21.82	0.10	21.62	0.15	21.40	0.12
V44	9.0970	–	21.10	21.80	0.10	21.27	0.10	–	–	–	–
V45	8.7620	–	21.50	22.05	0.10	21.36	0.10	21.04	0.19	–	–
V57	7.2595	–	21.35	21.70	0.10	–	–	–	–	–	–
V64	19.5745	19.57070	21.05	21.79	0.04	20.93	0.04	20.44	0.32	20.02	0.25
V72	8.6805	9.09400	21.72	22.32	0.04	21.76	0.04	21.34	0.26	21.02	0.20
V77	5.8170	–	22.10	22.60	0.10	22.00	0.10	–	–	–	–
V79	8.2480	–	21.95	22.55	0.10	21.70	0.10	–	–	–	–
V81	19.9570	–	21.15	21.88	0.10	21.12	0.10	–	–	–	–
V92	13.3165	–	21.45	21.93	0.10	21.15	0.10	–	–	–	–
P1	–	8.61700	22.30	22.99	0.05	22.28	0.05	22.07	0.30	21.76	0.23
P2	–	5.27800	22.00	22.50	0.04	22.18	0.04	22.10	0.22	21.87	0.17
P3	–	13.60000	21.50	22.00	0.03	21.24	0.03	20.77	0.22	20.36	0.17
P4	–	2.32980	22.55	23.13	0.04	23.06	0.06	–	–	–	–
P5	–	10.62600	21.60	22.30	0.04	21.64	0.04	20.91	0.30	20.30	0.24
P6	–	4.70380	21.65	22.23	0.03	21.68	0.04	21.40	0.25	21.00	0.20
P7	–	5.34060	22.31	23.00	0.04	21.65	0.04	–	–	–	–
P8	–	2.54200	22.71	23.07	0.03	22.79	0.04	–	–	–	–
P9	–	5.34250	21.74	22.42	0.04	21.73	0.04	20.93	0.30	20.61	0.23
P10	–	3.20620	21.85	22.63	0.04	21.68	0.05	21.13	0.34	20.53	0.26
P11	–	2.78930	21.10	22.00	0.05	21.58	0.06	21.12	0.40	–	–
P12	–	10.85540	21.80	22.57	0.04	22.27	0.05	21.86	0.34	–	–
P13	–	6.00240	21.89	22.33	0.03	21.81	0.04	21.26	0.19	21.00	0.15
P14	–	17.29510	22.20	22.65	0.03	–	–	22.09	0.20	–	–
P15	–	7.10590	21.10	21.80	0.04	21.30	0.04	21.19	0.31	–	–
P16	–	3.54310	22.70	23.41	0.06	22.89	0.06	22.32	0.31	21.85	0.24

^AThis error is an upper limit, in fact it is the half-amplitude of the light curve in this band, obtained using the information from the blue light curves (see Sect. 3 for details).

5. The distance modulus

5.1. The relative apparent distance moduli

Recently, it has been repeatedly pointed out that the principal source of systematic errors in the calibration of the primary distance indicators is in the uncertainty in determination of the zero points of the Cepheid Period-Luminosity and Period-Luminosity-Color (PLC) relations (Freedman & Madore 1993, Fukugita et al. 1993). For this reason we prefer to derive the distance modulus of NGC 3109 by comparison with the Large Magellanic Cloud Cepheids, as we did in the other papers of this series (CPB, PCP) and as it was originally suggested by F88. Indeed the distance modulus of the LMC can be derived using several independent methods (and owing to the large number of known Cepheids in the Magellanic Clouds, these galaxies represent almost ideal laboratories for the calibrations of PL and PLC relations). The method has the advantage of leaving the relative distance unaffected by whatever improvement there will be in the distance of the LMC. According to Hunter & Gallagher (1985), the metal content of NGC 3109 should be just ~ 1.5 times higher than in the LMC. Therefore, we do not expect significant effects on the PL relations for the two galaxies. In fact, Freedman & Madore (1990) have shown that the distance moduli obtained via Cepheid PL relation in a study of three fields of M31 with metal content from 0.5 to 2.5 times the solar metallicity range over less than 0.27 mag.

Figures 4, 5, 6 and 7 present the PL relations from the mean B , V , R and I magnitudes of the Cepheids listed in Table 5. *Filled circles* represent both SC and our Cepheids in the field F1 of NGC 3109, while *open circles* refer to the SC Cepheids located in the other fields. *Crosses* reproduce the photoelectric data for the LMC Cepheids (Sandage 1988, Madore & Freedman, 1991), shifted by the zero point difference between the NGC 3109 PL relation and the LMC one. The slopes of these two relations appear similar in all four colors, in agreement with the postulate on which the use of the Cepheids as distance indicators rests, i.e. that their properties are independent of the host galaxy (*cf.* also Section 7). For each color we built a PL relation with all the Cepheids (upper plot) and one in which we used only the Cepheids with a well defined light curve and a uniform phase coverage (referred to as “selected” from here on). This last selection allows us to include only those Cepheids with the most reliable light curve parameters as period, minimum, and mean magnitude.

In this paper, for consistency with CPB, we adopt a true distance modulus to the LMC of 18.50 mag (van den Bergh, 1996)³ and a mean total extinction to the LMC Cepheids $E(B - V) = 0.08$ mag (*cf.* discussion in CPB). Note that Bessel (1991) obtained a foreground reddening of the LMC which ranges from 0.04 to 0.09 mag, while the mean internal reddening is 0.06 mag, though in some regions it reaches values as high as 0.3 mag.

³We want note that the current best estimate of the distance modulus of the LMC is based on the light echo from the SN1987a ring. Panagia et al. (1997) give $\mu_0 = 18.58 \pm 0.03$ mag.

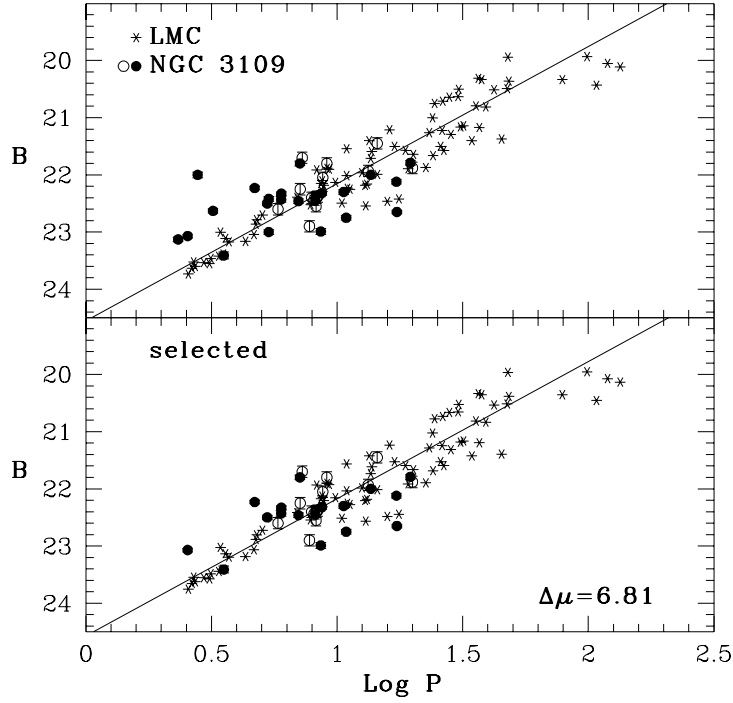


Fig. 4.— The Period-Luminosity relation in the B -band for the NGC 3109 Cepheids is compared with the corresponding relation for the LMC (from Sandage 1988 and Madore & Freedman, 1991). *Filled circles* represent both SC and our Cepheids located in the field F1 of NGC 3109, *open circles* the SC Cepheids located in the other fields. The magnitude error bars have dimensions of the order of the symbol size. *Crosses* reproduce the photoelectric data for the LMC Cepheids shifted by the zero point difference between the NGC 3109 and the LMC PL relations. In the *upper panel* all the variables are used, while in the *lower panel* only the Cepheids with the most reliable light curve parameters are plotted. A best fit (see text) of the selected sample to the LMC Cepheids with $\log P < 1.8$ gives us an apparent relative distance modulus $\Delta\mu_B = 6.81 \pm 0.11$.

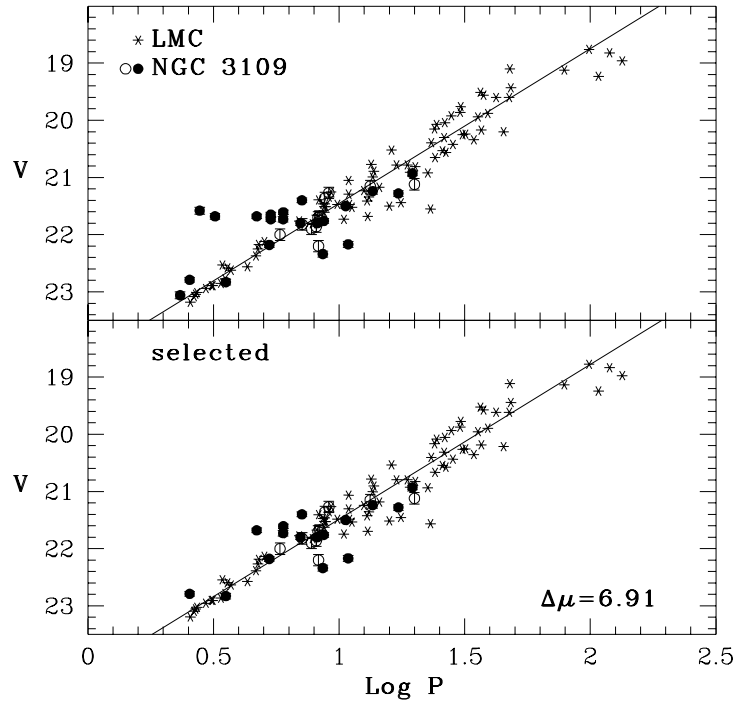


Fig. 5.— As in Fig. 4, but for the V -band. The resulting apparent relative distance modulus is $\Delta\mu_V = 6.91 \pm 0.09$.

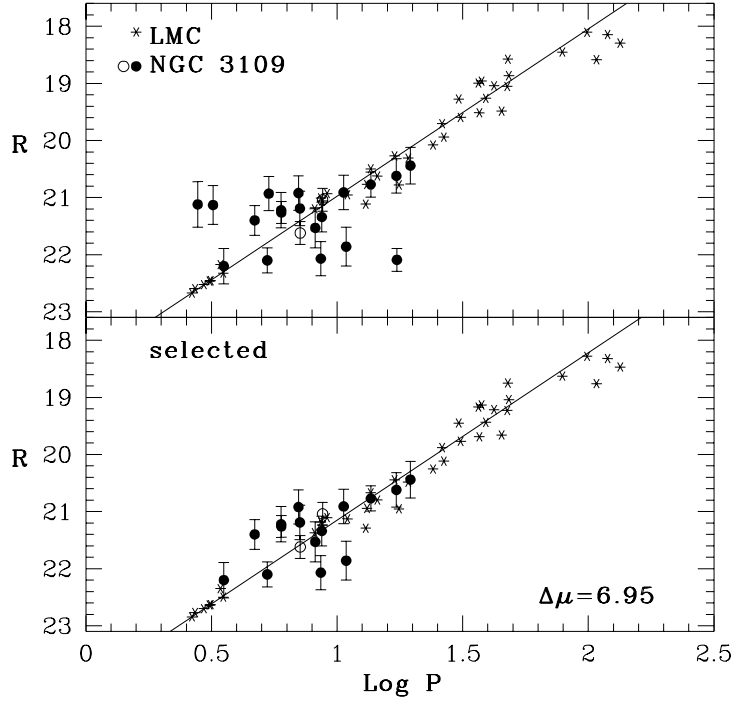


Fig. 6.— As in Fig. 4, but for the R -band (the plotted errors are an upper limit, see Sect. 4 for details). The resulting apparent relative distance modulus is $\Delta\mu_R = 6.95 \pm 0.13$.

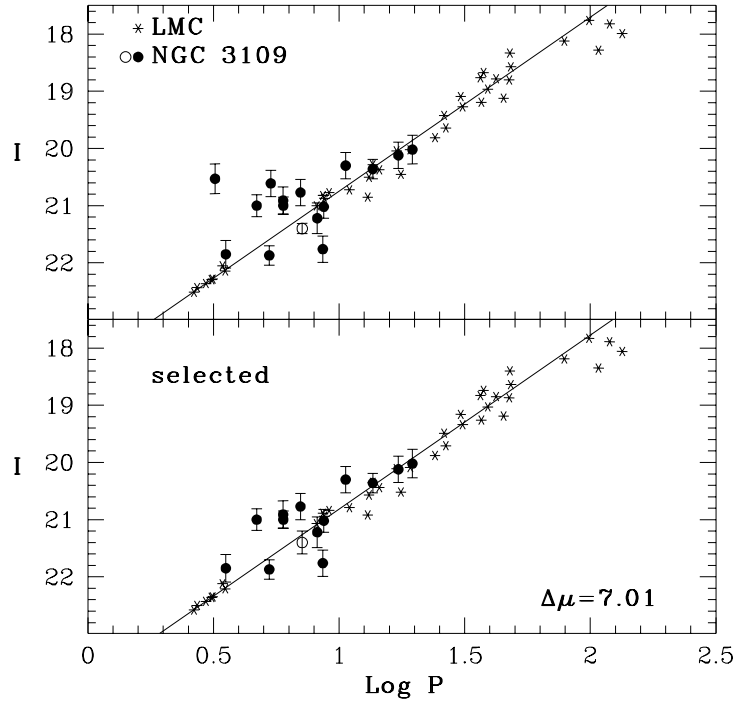


Fig. 7.— As in Fig. 4, but for the I -band (the plotted errors are an upper limit, see Sect. 4 for details). The resulting apparent relative distance modulus is $\Delta\mu_I = 7.01 \pm 0.12$.

In this picture, it is very difficult to estimate the mean total reddening of the sample of the LMC Cepheids. As it will be discussed below, the adopted reddening for the LMC has no effect on the determination of the relative (to the LMC) and absolute distance modulus of NGC 3109: it only affects the estimate of the total average reddening of its Cepheids.

In order to calculate the apparent distance moduli relative to the LMC in all four bands, we obtained the best fit (least squares method) for the PL relation of the LMC and then we calculated the best match of the PL relation of NGC 3109 imposing the same slope of the PL relation of the LMC. For an additional internal check of our results, we repeated these calculations using different approaches. First, we considered the two different samples of Cepheids in NGC 3109 defined above. Moreover, while the PL relation for the LMC was fitted with a straight line over the range of periods $0 < \log P < 1.8^4$, the two samples of NGC 3109 Cepheids were fitted both in the entire range of periods and in the range $0.8 < \log P < 1.8$ in order to minimize the effects of the Faint end selection bias in the small number data set of the more distant galaxy NGC 3109. The resulting relative distance moduli are all consistent within the errors. Thus we adopted the relative distance moduli obtained with the Cepheids of the selected sample of NGC 3109 without any constraint on $\log P$. In this way we make use of the same range of periods for both the LMC and NGC 3109, but we exclude those Cepheids with inaccurate parameters which might affect the reliability of the fit (almost all of them are in the fainter part of the PL relation). The resulting apparent distance moduli relative to the LMC ($\Delta\mu$) are reported in the Table 6. The total error on these apparent distance moduli is obtained adding in quadrature the error of the fit and the mean internal photometric error (obtained for each band as a mean of the errors in Table 2 up to magnitude 23.75).

5.2. The absolute distance modulus

In order to determine the true distance modulus (TDM= μ_0) to NGC 3109, the total (foreground plus internal) extinction for the Cepheids must be evaluated.

Taking advantage of the multicolor apparent distance moduli (see Table 6) and assuming that all of the wavelength dependence of these moduli is due to the extinction, it is possible to fit all the data simultaneously with an interstellar extinction law. In particular, we assume that the reddening law for the LMC and NGC 3109 is the same as in the Galaxy, and use the law derived by Cardelli et al. (1989, C89).

Figure 8 shows the relative distance moduli plotted as a function of the inverse wavelength characteristic of each band. As in F88, the estimated errors were scaled as a

⁴Cepheids with $\log P > 1.8$ are excluded from the least-squares fit since both the evolutionary status and the reddening of these longer period Cepheids are controversial.

Table 6. Distance moduli relative to the LMC.

Bandpass	$\Delta\mu$	Error
B	6.81	0.12
V	6.91	0.11
R	6.95	0.15
I	7.01	0.15

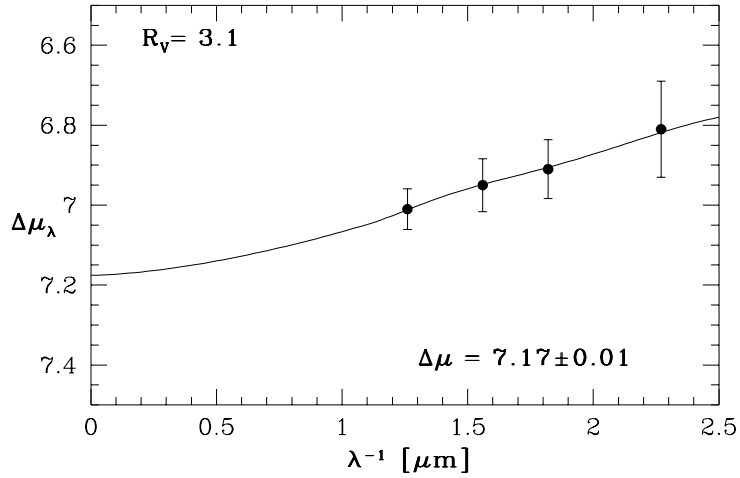


Fig. 8.— The NGC 3109 apparent distance moduli obtained in 4 bands are plotted as a function of the corresponding inverse wavelength (in μm^{-1}). A weighted least square fit of the Cardelli et al. (1989) extinction law (*solid curve*) leads to a true relative distance modulus $\Delta\mu_0 = 7.17 \pm 0.01$.

function of the increasing wavelength to reflect the decreasing strip width. The solid line is the weighted least square best fit of the adopted extinction law to the moduli. Following C89, we have adopted $R_V = A_V/E(B - V) = 3.1$, where A_V is the extinction in magnitudes in the V band. With this assumption, we obtained a reddening free relative distance modulus (RDM) $\Delta\mu_0 = 7.17 \pm 0.01$ and a relative reddening $\Delta E(B - V) = -0.09 \pm 0.02$ between the LMC and NGC 3109. This RDM corresponds to a TDM $\mu_0 = 25.67$, adopting $\mu_0 = 18.50$ for the LMC. A relative color excess $\Delta E(B - V) = -0.09$ would imply a negative total mean reddening (TR) $E(B - V) = -0.01$ for NGC 3109, if we assume, as discussed above and in CPB, $E(B - V) = 0.08$ for the total reddening of the LMC Cepheids. A negative reddening $E(B - V) = -0.07$ has been obtained by Freedman *et al.* (1992) for NGC 300. Of course, a negative reddening has no physical meaning, in terms of what we know about the interstellar medium. First, we must note that in our case the uncertainty on the $\Delta E(B - V)$ is of the order of 0.04 magnitudes (see below), and therefore we can assume that the TR is compatible with zero. Still, we would remain with the unlikely situation of a *zero* total extinction for the Cepheids in NGC 3109. There might be many explanations for such a result. Systematic calibration errors can play a role in the determination of the relative extinction, though we can exclude systematic errors larger than ~ 0.03 mag. Another interesting possibility is that the intrinsic color of the Cepheids in NGC 3109 is systematically bluer than those in the fiducial sample of the LMC, therefore leading to an underestimation of their reddening. However, we believe that the largest uncertainty is still on the adopted total reddening for the LMC. We have already discussed (previous Section) the difficulties in estimating the mean internal and external extinction toward the LMC Cepheids. According to Bessel’s (1991) results, the $E(B-V)=0.08$ mag for the LMC that we have adopted in this series of papers might be too low. The comparison between the LMC and NGC 3109 Cepheids seems to confirm that an $E(B - V)_{LMC} = 0.1$ mag (see also Freedman et al., 1991) or higher might be more appropriate.

The total error on the TDM of NGC 3109 is the combination of 1) the error on the best fit of the extinction law of C89, 2) the uncertainty on the absolute distance to the LMC, 3) the error on the photometric zero point, and 4) the error due to the assumption of $R_V = 3.1$.

The LMC best distance determination are based on the Cepheids (*cf.* the compilation of Feast & Walker, 1987), and the associated uncertainty is ± 0.15 mag; smaller errors seem too optimistic (see van den Bergh 1996). This is still the dominant source of errors. The uncertainty on the zero point calibration is ± 0.03 mag (a mean of the errors estimated in Sect. 2). Finally, C89 have shown that R_V can range from 2.75 to 5.3 within the Galaxy. Adopting this range in R_V for NGC 3109, the reddening value and the relative distance modulus would be in the interval $-0.01 < E(B - V) < 0.01$ and $7.16 < \Delta\mu_0 < 7.25$, respectively. In other words, a plausible error estimates for the distance modulus as a consequence of the extinction law uncertainties is ± 0.05 mag.

In summary, we have that the true distance modulus of NGC 3109 is $\mu_0 = 25.67 \pm 0.16$ mag and the total reddening is $E(B - V) = -0.01 \pm 0.04$ mag.

5.3. Reddening-free PL Relation

In the previous Sections we have used the information from several photometric bands and the fit of an interstellar extinction law to the data in order to make an extrapolation to infinitely long wavelengths and estimate the total extinction and the true distance modulus. However, even without solving explicitly for the reddening, it is still possible to obtain an estimate of the distance modulus which is independent of reddening. This can be done by defining the reddening-free magnitude $W = V - R_V \times (B - V)$ (Freedman et al., 1992).

Figure 9 displays the $W - \log P$ relation for NGC 3109 (selected sample) and for the LMC. From this relation we obtain a true relative distance modulus $\Delta\mu_0 = 7.23 \pm 0.20$ which is consistent with the true relative modulus obtained in the previous Section.

The disadvantage of this reddening-free method is that the uncertainties on the W magnitudes are larger than the single errors on the original B and V magnitudes, as W results from a combination of the two. For this reason we obtain an error on the true relative modulus which is one order of magnitude larger than that on the modulus obtained by the multiwavelength method. Moreover, W depends on two of the four available colors only, making the distance based on it statistically less accurate. For this reason we have constructed a new parameter W' analog to the W , but depending on R and I . The two reddening free parameters (W from B and V and W' from R and I) are statistically uncorrelated and could be used as a further, independent estimate of the distance modulus. W' was derived generalizing the definition of W , and applying it to the R and I bands. In fact, we can substitute the parameter R_V by $\mathcal{R}(R, I) = A_I/E(R - I)$, and then define the new parameter $W' = I - \mathcal{R}(I, R) * (R - I)$. $\mathcal{R}(I, R)$ can be easily derived by the C89 law. Figure 10 displays the $W' - \log P$ relation for NGC 3109 (selected sample) and for the LMC. From this relation we obtain a true relative distance modulus $\Delta\mu_0 = 7.19 \pm 0.20$ which is in a very good agree with that obtained from the $W - \log P$ relation. This result is a proof of the utility and reliability of this method. The use of both W and W' can be used as a test of self consistency, and a way of assessing external errors.

6. The Period-Color relation

In the Figs. 11, 12, and 13, we compare the Period-Color relations (PC) for the LMC and NGC 3109 for the three colors $(B - V)$, $(V - R)$ and $(V - I)$; for NGC 3109 the selected sample has been used (the errors for the colors $(V - R)$ and $(V - I)$ are larger because we use the maximum expected value and represent an upper limit, see Sect. 4 for details).

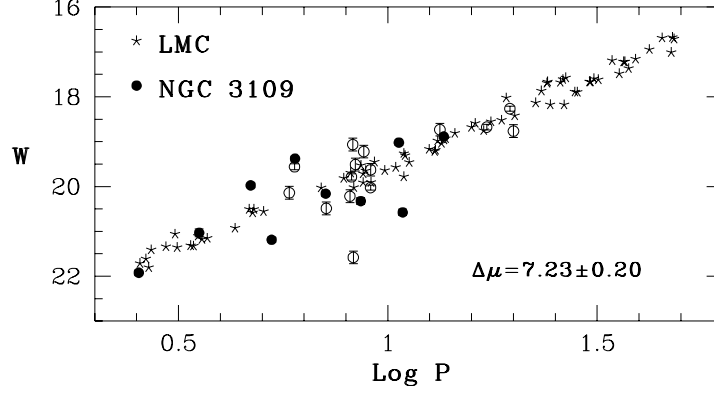


Fig. 9.— The reddening-free $W - \log P$ relation for the NGC 3109 Cepheids (*open circles* for the original SC variables and *filled circles* for the new candidates), compared to the LMC Cepheids (*crosses*). The corresponding true relative distance modulus is $\Delta\mu = 7.23 \pm 0.20$.

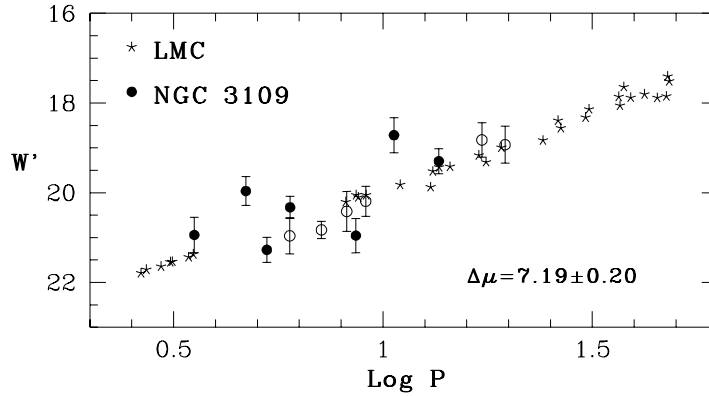


Fig. 10.— As in fig. 10, but for the new reddening-free $W' - \log P$ relation (see Sect. 5.3 for details) The corresponding true relative distance modulus is $\Delta\mu = 7.19 \pm 0.20$.

In each figure, the data in the *upper panel* are without reddening correction and those in the *lower panel* are corrected according to the reddening effects. The Fig. 14 shows the same three absorption-corrected PC relations for the LMC, NGC 3109, Sextans A (PCP), Sextans B (PCP), and IC 1613 (F88). The slopes of these PC relations are the same, within the uncertainties. The data of NGC 3109, Sextans A, Sextans B, and IC 1613 have a larger scatter than for the LMC, consistent with the lower accuracy in the determination of the mean magnitudes.

In order to obtain the zero point difference between the PC relations for the LMC and the other galaxies, the LMC PC relations were fitted with a straight line over the range of periods $0 < \log P < 1.8$, and a linear fit of the PC relations was performed for the other galaxies imposing the same slope of the LMC. In this way we could calculate the mean color difference between the Cepheids in the LMC and in the other four galaxies. Figure 15 shows that the mean color difference after the reddening corrections is consistent with zero. This result shows that, if we suppose that the colors of the Cepheids are independent of the parent galaxy, the law by C89 allows to calculate relative reddenings in a consistent way.

With the data set presented in this paper, we can check whether the Cepheids in NGC 3109 have the same average colors as in the LMC. Figure 16 displays the reddening-free parameter $Q = (B - V) - [E(V - I)/E(B - V)](V - I)$ as a function of $\log P$ for both the selected sample of Cepheids in NGC 3109 (*filled circles*) and in the LMC (*crosses*) (see Freedman *et al.*, 1992). The slopes of the two distributions are the same as well as the zero point. The larger scatter for the NGC 3109 Cepheids is consistent with the larger photometric errors. The similarity of these two distributions suggest that the colors of the Cepheids in these galaxies are the same.

Finally, in Fig. 17 we compare the amplitude of the B light curves of the Cepheids in NGC 3109 and in the LMC. Also in this case we obtain that the trend and the dispersion of the points for the two populations of Cepheids are similar, suggesting similar properties.

7. Conclusion

In conclusion, an extended PL relation and the multicolor photometry provide a new, more accurate, de-reddened distance of NGC 3109 relative to the LMC. Adopting $\mu_0 = 18.50$ for the LMC, we obtain a true distance modulus $\mu_0 = 25.67 \pm 0.16$ for NGC 3109; if we assume a reddening $E(B-V)=0.08$ for the LMC, the total reddening of the Cepheids in NGC 3109 is $E(B - V) = -0.01 \pm 0.04$. The new reddening free distance modulus corresponds to 1.36 ± 0.10 Mpc.

This new distance is consistent, within the errors, with the value $\mu_0 = 25.5 \pm 0.2$ given by CPB, though, formally, now NGC 3109 is placed $\sim 7\%$ further away. It is instructive to inspect the origin of this difference. In CPB we had only B and V-band data. It was difficult

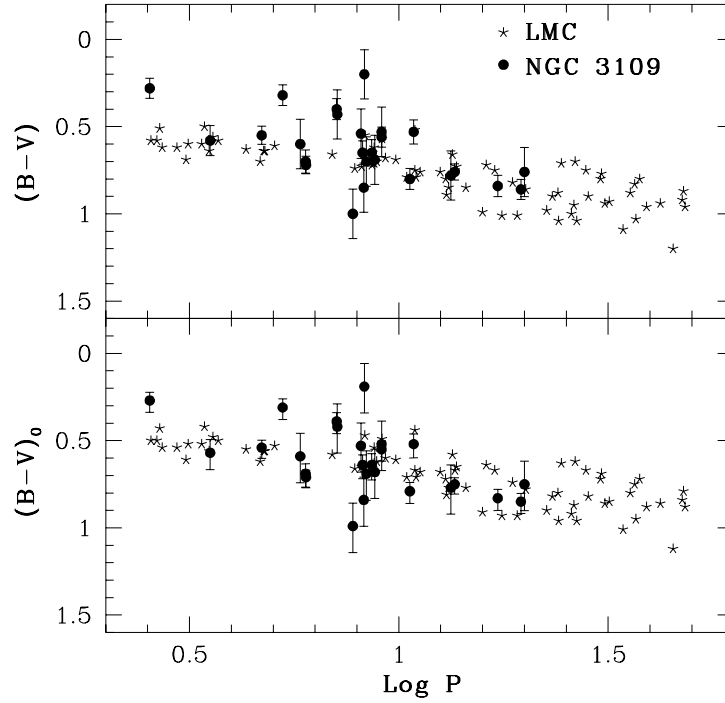


Fig. 11.— The $(B-V)$ colors for the Cepheids in the LMC (*crosses*) and in NGC 3109 (*filled circles*) are plotted against the logarithm of the period in days. For NGC 3109 we draw also the errors over the determination of the colors. The *upper panel* shows the data without any correction for the reddening, while the *lower panel* displays the absolute colors [adopting $E(B-V)=0.08$ for the LMC]. For NGC 3109 we use $E(B-V)=0.0$ (see text for details). The trends of the two populations is remarkably similar. The larger scatter in NGC 3109 is due to the larger errors in the determination of the mean magnitudes.

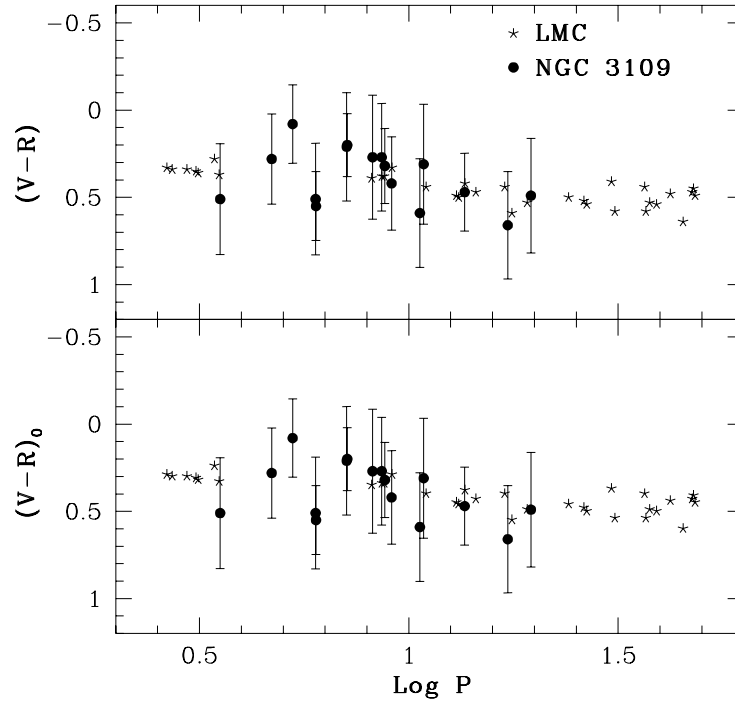


Fig. 12.— As in fig. 11, but for the $(V - R)$ colors (the plotted errors are an upper limit, see Sect. 4 for details).

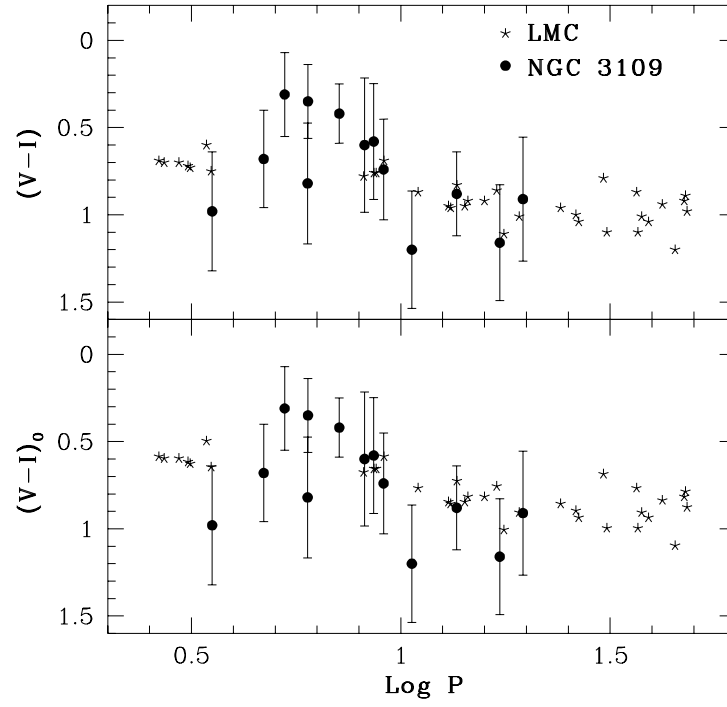


Fig. 13.— As in fig. 11, but for the $(V - I)$ colors (the plotted errors are an upper limit, see Sect. 4 for details).

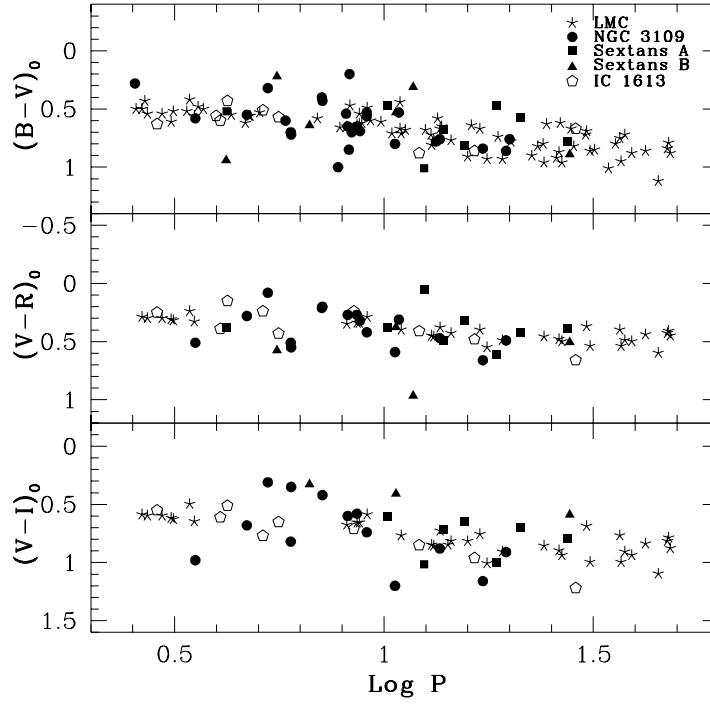


Fig. 14.— Period-Color relation after the correction for reddening for the LMC, NGC 3109, Sextant A, Sextant B and IC 1613. As for NGC 3109, the large scatter for Sextant A and Sextant B is due to the larger errors in the determination of the mean magnitudes.

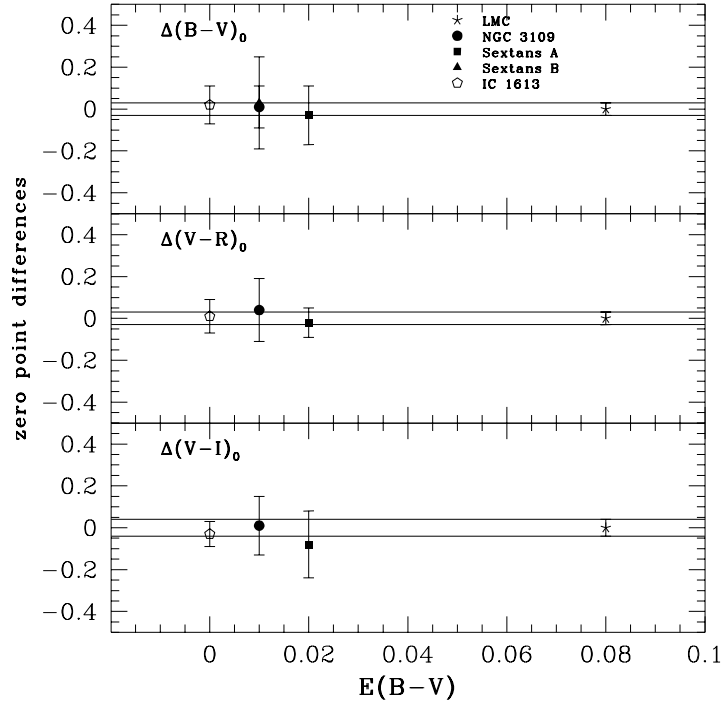


Fig. 15.— The zero point difference (after reddening correction) between the *PC* relations in (B-V), (V-R), and (V-I) for the LMC and for NGC 3109, Sextans A, Sextans B, and IC 1613 is plotted against the reddening. The *cross* is the LMC and the two lines represent the range of errors for the LMC zero point.

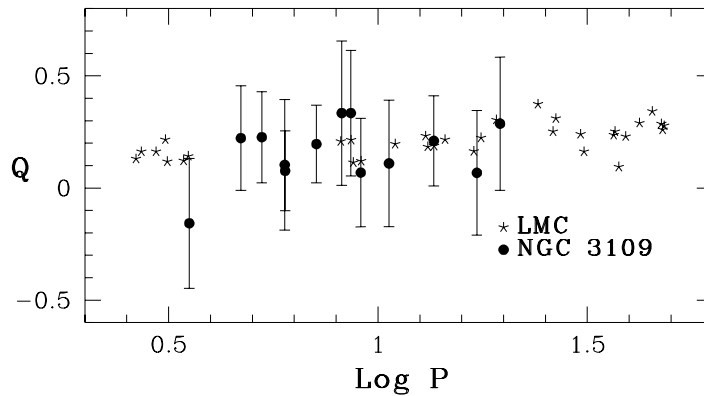


Fig. 16.— The reddening-free parameter $Q = (B - V) - [E(V - I)/E(B - V)](V - I)$ is plotted as a function of $\text{Log } P$ for both the selected sample of Cepheids in NGC 3109 (*filled circles*) and in the LMC (*crosses*). The widths and the slopes of the two distributions are the same as well as the zero point. The larger scatter for the NGC 3109 Cepheids is consistent with the larger photometric errors (for the magnitude I the error considered is an upper limit, see Sect. 4 for details).

to apply the multiwavelength method to this data set, in view of the closeness of the two bands and of the poor coverage in the V band. For this reason, CPB preferred to adopt a mean reddening $E(B-V)=0.04$ for NGC 3109 and estimate the true distance modulus with this assumption in mind. The reddening estimate (from Burstein & Heiles, 1992) contour maps was admittedly poor (as noted also by BPC). The difference between the reddening adopted by CPB and the present direct estimate of the mean reddening toward NGC 3109 completely explains the difference in the final absolute modulus. As further evidence, we can refer to the exercise presented by Piotto et al. (1995), where we used the two B and V apparent relative distance moduli of NGC 3109 for a rough estimate of the true relative distance moduli with the multiwavelength method applied also in the present paper. Even with a poorer data set Piotto et al. (1995, cf. their Fig. 2) obtained a true relative distance modulus $\Delta\mu_0 = 7.23 \pm 0.10$, much closer to the present estimate. This discussion shows by itself the importance of extending the Cepheid light curves to the largest possible wavelength interval. For this reason, we are observing these same Cepheids of NGC 3109 in the JHK bands. We expect to reduce the error in the distance and reddening estimate. For the importance of the JHK observations of Cepheids, see Madore and Freedman (1991)

Finally, we want to briefly comment on the similarity of *(i)* the slopes of the Cepheid PL and PC relations, *(ii)* the average color, and *(iii)* of the properties of the amplitude-period relations which result from a direct comparison of the data from five galaxies (cf. discussion in Section 5.1, and 6). This is consistent with the fundamental assumption on which the entire extragalactic distance scale stands. However, we must also point out the large uncertainties still present in the determination of all the above parameters (*cf.* also the discussion in Section 5.2), in part as a consequence of the nature of this kind of research, which requires a huge amount of telescope time. It is clear that the dispersion (intrinsic and as a consequence of the observational uncertainties) of the relations presented in Figs. 4-7, and in Figs. 11-17 are too large for a firm conclusion on the universality of the Cepheid properties. A lot of work on the theoretical and observational side is still needed. In particular, we must take advantage of the recent improvement in the near-IR detectors, where the PL and PLC relations are much narrower.

We wish to thank Wendy Freedman for providing us with her LMC Cepheid data set in a computer readable form and Barry Madore for the useful comments. The authors acknowledge the support by the Agenzia Spaziale Italiana. IM acknowledges the partial support of the Istituto Italiano per gli Studi Filosofici, Napoli.

REFERENCES

- Bessel, M.S. 1991, A& A, 242, L17
- Bresolin, F., Capaccioli, M., Piotto, G. 1993, AJ, 105, 1779 (=BCP)
- Burstein, D., Heiles, C. 1982, AJ, 87, 1165
- Capaccioli, M., Piotto, G., Bresolin, F. 1991, AJ, 103, 1151 (=CPB)
- Cardelli, J.A., Clayton, G.C., Mathis, J.S. 1989, ApJ, 345, 245 (=C89)
- Feast, M.W., Walker, A.R. 1987, ARA& A, 25, 345
- Freedman, W.L. 1988, ApJ, 326, 691 (=F88)
- Freedman, W.L., Madore, B.F. 1990, ApJ, 365, 186
- Freedman, W.L., Grieve, G.R., Madore, B.F. 1985, ApJS, 53, 311 (=F85)
- Freedman, Madore, B.F., Hawley S.L., Horowitz I.K., Mould J., Navarrete M., Sallmen S.
1992, ApJ, 396, 80
- Freedman, W. L., Madore B., 1993, IAU Coll., 139, 61
- Freedman, W.L., Wilson, C.D., Madore, B.F. 1991, ApJ, 372, 455
- Fukugita et al., 1993, Nature, 366, 509
- Landolt, A.U. 1983a, AJ, 88, 439
- Landolt, A.U. 1983b, AJ, 88, 853
- Landolt, A.U. 1992, AJ, 104, 340
- Panagia, N., Gilmozzi, R., Kirshner, R.P., 1997, in *SN 1987A: Ten Years After*, in press
- Pellegrini, C., Laureato Thesis, Università di Padova
- Piotto G., Capaccioli, M., Pellegrini, C. 1994, A& A, 287, 371
- Piotto, G., Capaccioli, M., Musella, I., D’Onofrio, M., Planetary and Space Science, 1995,
43, 1405
- Sandage, A., Carlson, G. 1982, AJ, 258, 439
- Sandage, A., Carlson, G. 1985, AJ, 90, 1019
- Sandage, A., Carlson, G. 1988, AJ, 96, 1599 (=SC)

Saha, A., Hoessel, J.G. 1990, AJ, 99, 97

Saha, A., Labhardt, L., Schwengeler, H., Macchetto, F.D., Panagia, N., Sandage, A.,
Tamman, G.A. 1994, ApJ, 425, 14

Stetson, P.B. 1987, PASP, 99, 191

van den Bergh, S., 1996, Dahlem Workshop Report

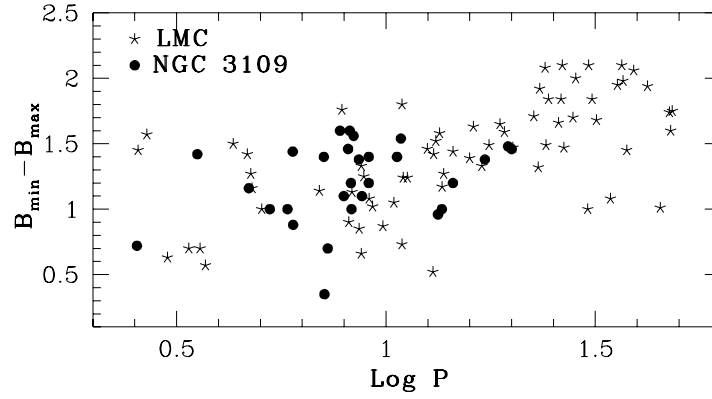


Fig. 17.— The light curve amplitudes ($B_{\min} - B_{\max}$) for the LMC (*crosses*) and NGC 3109 (*filled circles*) Cepheids are plotted against the logarithm of the period in days. The trend of the two populations of Cepheids is remarkably similar, suggesting similar properties.